A Multi-Body Implementation of Finite Volumes C^0 Beams

Gian Luca Ghiringhelli[1], *Pierangelo Masarati and Paolo Mantegazza*

Dipartimento di Ingegneria Aerospaziale

Politecnico di Milano

via C. Golgi 40 - 20133

MILANO - Italy

Abstract. The paper describes an unusual C^0 beam discretization based on the finite volumes concept. In the linear case this approach leads to a collocated evaluation of the stiffness matrix of the beam and it proves to be intrinsically free from shear locking. In the non-linear formulation, only a collocated evaluation of the elastic forces is required, that dramatically simplifies the computation of the elastic contribution to the equilibrium equations. The formulation is here developed for the general geometrically non-linear case and implemented in Multi-Body formulation. The proposed approach proved to be consistent; its major drawback lies in the loss of symmetry of both the linear and the linearised beam matrices. For this reason the method happens to be particularly suitable for dynamic problems like a non-linear implicit multi-body numerical approximation, in which the symmetry of the matrices is not so important, as it is already lost, while the ease in the generation of the contributions to the equations may lead to faster and cheaper analyses. Some applications are outlined and the most relevant results are discussed.

Keywords: Beams, Finite Volumes, Multi Body Dynamics

Introduction

Beams are quite an important tool in structural analysis, since they represent a relatively simple model compared to a three dimensional analysis of slender structural systems. The finite element method found its first application in trusses and frames structural analysis; nowadays the numerical analysis of beam structures still retains

[1]Corresponding author,
Tel.: ++39+2-2399-4056
Fax: ++39+2-2399-4034
E-mail: *ghiringhelli@aero.polimi.it*

its importance and beam elements play an important role in almost all the commercially available F. E. codes. A great effort has been made by many researchers to deepen the knowledge on the subject. The characterisation of the elastic behaviour of the beam section has been treated by, among others, Giavotto *et al.* [1], Bauchau [2], Hodges [3], Ghiringhelli and Mantegazza [4], Borri *et al.* [5], while the three-dymensional behaviour, with particular regard to the dynamic response, has been comprehensively studied in a large number of works, among which mention should be made of those by Bathe, [6], Borri and Merlini [7], Simo [8], [9], Borri *et al.* [10], [11] and Ghiringhelli [12]. An important class of beam models is represented by C^0 beams. They result from the removal of the oversimplifying assumption on the shear deformation that characterises Euler beams. However such a beam model is known to suffer from shear locking when low order shape functions are used to interpolate nodal displacements and rotations [13]. The locking may be overcome in many ways, ranging from relaxed integration to strain-based formulations [12]. The proposed method, based on the Finite Volumes concept, represents an interesting solution. Finite volumes are widely used in fields like computational fluid dynamics and heat transfer, while their use in structural analysis has been limited by the diffusion of well suited variational principles. As previously stated, the variational approach is known to suffer from shear locking; the finite volumes approximation instead proved to be intrinsically shear lock free [14]. So it is worth to explore the possibility of extending such a formulation to geometrically non linear beams to be used within multi-body formulations, where the loss of symmetry of the stiffness matrix is not important as other contributions determine the loss of symmetry anyhow [15], [16].

Finite Volumes Formulation

Differential Equilibrium Equation

The beam is defined by means of a regular reference line p, which maps the one-dymensional domain B to the three-dimensional space, that is $p : B \subset \Re \mapsto \Re^3$. The position of an arbitrary point $p(\xi)$ on the beam reference line is identified uniquely by means of an abscissa $\xi \in B$. The equilibrium equation of the beam is stated in terms of internal forces ϑ and external (imposed) loads τ:

$$\vartheta' - T^T \vartheta + \tau = 0 \tag{1}$$

where derivation occurs with respect to the abscissa ξ; matrix T is defined as follows:

$$T = \begin{bmatrix} 0 & p'\times \\ 0 & 0 \end{bmatrix}$$

and represents the arm of the internal force in the differential equilibrium equation of moments. It descends from the axiomatic assumption according to which the density of strain power due to a rigid motion vanishes. In fact, the strain power density for a beam may be written as follows:

$$\Pi_s = (v \cdot t)' + (\omega \cdot m)' \tag{2}$$

where t and m are respectively the shear force and the bending couple (i.e. $\vartheta = \{t, m\}$), and v and ω are the linear and spin velocities of an arbitrary point of the beam. Without any loss in generality, they may be written as follows:

$$v = v_r + \omega_r \times p, \qquad \omega = \omega_r \tag{3}$$

where v_r, ω_r are the "rigid" velocities that describe the rigid motion. Then the strain power density, Equation (2), due to the rigid motion of Equations (3), becomes:

$$\Pi_s = \omega_r \cdot (p' \times t + m') + v_r \cdot t' = 0 \tag{4}$$

For sake of simplicity, Equation (4) has been evaluated at point $p = 0$ due to the arbitrariness of the rigid displacement. The expressions that multiply the rigid motion velocities in Equation (4) are the true internal forces that participate in the differential equilibrium in Equation (1). The corresponding generalised deformations vector, made of the strains ε and the curvatures κ, will be called ψ: $\psi = \{\varepsilon, \kappa\}$. Internal forces and deformations are related by means of a constitutive law. Under the assumption of linear strains, which can be considered as acceptable if the strains remain small even when the structure undergoes large displacements and rotations, the components of ψ can be related to the internal forces ϑ by means of a linear elastic constitutive law, i.e.:

$$\vartheta = D\psi \tag{5}$$

where D plays the role of an arbitrary[2] sectional stiffness matrix. The proposed formulation may be extended in a straightforward manner to the case of an arbitrary constitutive law. Anyway, apart from a few significant exceptions, when a

[2]The only constraint is due to the consideration that if a purely elastic constitutive law is to be considered, it must be able to represent a conservative strain energy.

beam structure goes beyond the linear elastic behaviour, its model may lose its appeal, since a deeper analysis of local non-linear costitutive *phænomena* is required. Refs. [1], [4] present a semi-analytical formulation based on the discretisation of the beam section in a finite elements sense. This formulation allows the numerical determination of the coefficients of the linear elastic constitutive law for fully anisotropic, non-homogeneous beam sections, thus allowing the modelling of a wide variety of non conventional beams.

Finite Equilibrium: Weighted Residuals Interpretation

The finite volumes approach may be interpreted, in a mathematical sense, as a weighted residuals weak formulation of the finite equilibrium. Let's consider Equation (6), which comes straightforward from Equation (1):

$$\int_a^b w \left(\vartheta' - T^T \vartheta + \tau \right) \, d\xi = 0 \tag{6}$$

The weight function w is $w = \text{step}\left(\xi - a\right) - \text{step}\left(\xi - b\right)$ and assumes unit value inside domain $[a, b]$. It owns the following properties:

$$\left.\begin{array}{l} w = 0 \\ w' = 0 \end{array}\right\} \; \xi = [-\infty, a^-], \; \xi = [b^+, +\infty] \qquad \left.\begin{array}{l} w = 1 \\ w' = 0 \end{array}\right\} \; \xi = [a^+, b^-]$$

$$\left.\begin{array}{l} w = 1/2 \\ w' = \infty \end{array}\right\} \; \xi = a \qquad \left.\begin{array}{l} w = 1/2 \\ w' = -\infty \end{array}\right\} \; \xi = b$$

$$\int_{-\infty}^{\infty} f w' \, d\xi = f\left(a\right) - f\left(b\right)$$

that is $w' = \delta\left(\xi - a\right) - \delta\left(\xi - b\right)$, where δ is Dirac's impulse function. By means of integration by parts, Equation (6) leads to the following finite equilibrium relation:

$$\left(I - \int_{\xi_0}^{\xi} T^T \, d\eta \right) \vartheta \Big|_a^b = \; - \int_a^b w \left(I - \int_{\xi_0}^{\xi} T^T \, d\eta \right) \tau \, d\xi \tag{7}$$

In an heuristic sense the finite volumes approach describes the equilibrium of a finite piece of beam. In fact Equation (7) states that the internal forces at the ends of the piece of beam under analysis must balance the sum of all the external loads. Concentrated loads may be easily taken into account by means of Dirac functions in distributed loads τ. The integration of matrix T leads to:

$$\int_{\xi_0}^{\xi} T \, d\xi = \left[\begin{array}{cc} 0 & \left(p\left(\xi\right) - p\left(\xi_0\right)\right) \times \\ 0 & 0 \end{array} \right] = U\left(\xi\right) - U\left(\xi_0\right)$$

which represents the arm by means of which (internal and imposed) forces contribute to the equilibrium equation of moments. Eventually Equation (7) can be written as:

$$\left(I - U^T(\xi)\right)\vartheta\Big|_a^b = -\int_a^b w\left(I - U^T(\xi) + U^T(\xi_0)\right)\tau\, d\xi \tag{8}$$

The points that bound the arbitrary finite piece of beam have been called "evaluation points" [14]. The internal forces of the beam must be evaluated only in these points; this represents an high simplification in the determination of the contribution of the beam to the equilibrium equations. It is interesting to note that Equation (8) really is an equilibrium equation in terms of forces and couples, and thus could be written directly, without any "mathematical" interpretation. In its left hand side we have the contribution of the internal forces at the ends of the piece of beam, while on the right hand side we have the contribution of the external loads. Symmetry is lost due to arm matrix U that premultiplies the internal forces. When the dependance of the internal forces on the strains is expressed by means of the linear constitutive law presented in Equation (5), a finite equilibrium equation in terms of strains and curvatures at the evaluation points may be explicitly written, thus leading, in the linear simplification, to the usual finite beam stiffness matrix.

Generalised Strains

The generalised strains may be expressed in terms of derivatives of the position and the rotation of the sections with regards to their initial configuration. The strains in the global reference frame are defined by:

$$\varepsilon = p' - R\overline{p'}$$

where the rotation matrix R represents a rigid rotation from the initial configuration of an arbitrary section to its current one. Overlined quantities denote the initial values of the related entities. It should be noted that since the material constitutive matrix, Equation (5), is usually known in the material frame, the deformations ought to be translated in that frame in order to obtain the proper internal forces. Then the strains in the material frame become:

$$\tilde{\varepsilon} = R^T\varepsilon = R^T p' - \overline{p}'$$

where the tilde $\tilde{(\cdot)}$ denotes the entities translated in the material frame. The rotation strains, i.e. the elastic curvatures, are expressed by:

$$\kappa\times = R'R^T - R\overline{\rho} \times R^T \tag{9}$$

Matrix $R'R^T = \rho\times$ stands for the actual curvature, while $\overline{\rho}\times$, if any, stands for the curvature of the undeformed beam. The transformation from the actual to the material frame leads to:

$$\tilde{\kappa}\times = R^T R' - \overline{\rho}\times = R^T\rho \times R - \overline{\rho}\times$$

It should be noted that the presented definition of strains and curvatures, together with the previously written differential euqilibrium equation, stands for an intrinsic characterisation of the beam as a one-dimensional *continuum*. Thereby, the formulation is implicitly valid for initially curved and twisted beams, even if these are taken into account only in a discrete manner, since a collocated evaluation of strains, internal forces and constitutive properties is given.

A Noticeable Load Case: Inertia Forces

Inertia forces and couples represent a noticeable load case due to their importance in the dynamics of structures. They express a relation between configuration, i.e. the time derivatives of the displacements, and loads, thus suggesting interesting parallels with the constitutive law. Consistent inertia loads for the proposed formulation may be easily expressed. Let the inertia loads of an arbitrary section be represented by vector $\tau_{in.}$, which is defined as follows:

$$\tau_{in.} = \mathcal{M} \left\{ \begin{array}{c} \ddot{p} \\ \dot{\omega} \end{array} \right\}$$

where $\mathcal{M}$ is the inertia matrix of the section and $\ddot{p}$, $\dot{\omega}$ are the linear and angular accelerations of the section itself. Thus the contribution of the inertia of the finite piece of beam to the equilibrium equation, Equation (8), is:

$$F_{in.} = \int_a^b \left(I - U^T(\xi) + U^T(\xi_0)\right) \mathcal{M} \left\{ \begin{array}{c} \ddot{p} \\ \dot{\omega} \end{array} \right\} d\xi \tag{10}$$

It is apparent from Equation (10) that the finite inertia matrix is unsymmetric due to the premultiplication of the forces times matrix U^T. The importance of this term will be illustrated later.

Finite Volumes Multi-Body Implementation

The proposed formulation has been implemented in a Multi-Body code. Typical applications of Multi-Body formulations may be found in the dynamics of mechanisms as well as in large space structures modelling, like space orbiting stations, opening of solar arrays and towing of tethered satellites. Perhaps the most challenging aeronautical application is represented by the analysis of rotorcrafts. An instance of a Multi-Body analysis program, named MBDyn, has been developed at the Department of Aerospace Engineering of the *Politecnico di Milano*. The mentioned code is based on a time-integration kernel for the implicit step integration of mixed algebraic and first and second order differential equations. It performs unconditionally A-L stable implicit integration with very good precision. It may be classified as a "Lagrangian Multiplier" or "Redundant Coordinate Formulation" method, since it uses the six position and rotation degrees of freedom of each body as unknown, plus the internal unknown reaction forces that are related to each constraint equation that is considered. Moreover, the possibility of simultaneously solving differential equations of different order permits to avoid tedious and error prone usage of relations occurring between spin acceleration and rotation parameters, as will be shown later. As a consequence, three more degrees of freedom per body are added, namely the spin velocities, involving an increase in the dimensions of the problem. Since these extra degrees of freedom are fully uncoupled from the others, the management of matrix sparsity gives great advantages, leading to high numerical efficiency. Rotational equilibrium equations then become differential of the first order both in the spin velocity ω and in the rotation parameters. On the contrary, the translational equilibrium equations remain differential at the second order in the displacements.

Large Rotations

Let φ be a vector in a three dimensional domain: $\varphi \in \Re^3$. Matrix R represents a rotation φ_Δ of vector φ from its initial position φ_0 to position φ_1: $\varphi_1 = R\varphi_0$. Since the trigonometric functions in matrix R may cause some numeric ineffectiveness, the purely algebraic modified Gibbs-Rodriguez rotation parameters g are used in the present formulation instead of the rotational vector φ. They are defined as

$g = 2\,\tan(\varphi/2)$. The transformation matrix takes the following form:

$$R = I + \frac{4}{4 + g \cdot g}\left(g \times + \frac{1}{2} g \times g \times\right)$$

This transformation is singular for rotations that are integer multiples of π angle, but this causes no problems if an incremental solution process is used (Updated Lagrangian). Then matrix R contains the reference rotation, while the rotation unknowns are the Gibbs parameters that represent the incremental rotation from the reference configuration R_0 to the new one R_1 at the beginning of the integration step. Thus the difference between the two configurations is always sufficiently small at the end of the step for an acceptable accuracy so that no singularity results. The unknown variation in rotation may be granted indifferently by the parameters φ or g. An exaustive description of the rotation parameters properties, together with plenty of significant relations concerning with them, may be found in Refs. [17]. The kinematic unknowns of an arbitrary node and their time derivatives are thus given by the following expression:

$$q = \left\{ \begin{array}{c} x \\ g \\ \omega \end{array} \right\}, \qquad \dot{q} = \left\{ \begin{array}{c} \dot{x} \\ \dot{g} \\ \dot{\omega} \end{array} \right\}, \qquad \ddot{q} = \left\{ \begin{array}{c} \ddot{x} \\ 0 \\ 0 \end{array} \right\}$$

where x are the total coordinates of the node, g are the parameters describing a finite rotation from the reference frame at the last completed iteration to the (unknown) frame at the end of the running iteration, and ω are the spin velocities of the point. Every rigid body owns a q vector with nine unknowns and nine equations, six assessing the equilibrium of forces and couples at the node and three representing a constitutive relation between the time derivatives of rotation parameters and angular velocities. Reaction unknowns, if needed, may be added by means of equations that describe the constraint relations. The resulting system of equations is Differential Algebraic (DAE) of index three [18] and is solvable to the desired accuracy under relatively loose conditions.

Finite Volumes Multi-Body Beam Element

The proposed finite volumes beam element has been developed in order to give the code the capability to model the elastic deformation of bodies undergoing large displacements and rotations. According to the program philosophy, deformable beams

may be considered as elastic constraints that link otherwise independent rigid bodies. The finite volumes approach proved to be quite suitable for this interpretation, as it leads to collocated evaluation of the elastic forces, in opposition to rather more sophisticated variational methods which require (numerical) integration in some energetic sense [13]. A three node beam element has been implemented. A sketch can be found in Figure 1. This choice was dictated by the consideration that such an element in the linear case, with a proper choice of the evaluation points, proved to supply the exact solution for end applied loads [14], thus satisfying a sort of "minimal" requirement. A beam element is partitioned in three subparts, that are related to its reference points. These points in turn are related to geometrical nodes, that represent the main degrees of freedom of the problem, by means of an offset f. This versatility has been adopted to allow an easier definition of the beam element when the line that is suitable to describe the elastic behaviour of the beam section differs from the one that conveniently describes the mass distribution. Every node is characterised by its position and rotation matrix. A reference line describes the position of a reference point arbitrarily taken on the beam section; the configuration of the section at an arbitrary location ξ is described by a rotation matrix $R(\xi)$. Thus the reference line is not required to have some physical meaning. Every value of the abscissa ξ corresponds to a point p in a three dimensional domain: $p(\xi) : B \subset \Re \mapsto \Re^3$. The direction e_1 of the section reference frame is normal to the section; directions e_2, e_3 are mutually orthogonal, are normal to e_1 and lie in the section plane. The unit vector e_1 ought not to be tangent to the beam reference line, i.e. $dp/d\xi$: this allows the existence of the shear deformation. The section plane defined by the reference frame doesn't account for warping, which is assumed not to be affected by large displacements. This means that the second order work made by large displacements warping may be neglected (see Ref. [7]).

Generalised Deformations

The beam generalised strains have been previously defined. In the spirit of the above mentioned Updated Lagrangian approach to the rotation parameters, the curvatures may be expressed in terms of updated rotation parameters g as follows

straightforward from the derivation of matrix R, Equation (9):

$$\kappa\times = (Gg') \times + R_\Delta \kappa_r \times R_\Delta^T$$

Matrix R_Δ represents the variation of rotation matrix that occurs during the running iteration, thus being $R = R_\Delta R_r$. Only matrix R_Δ depends on the rotation parameters g, while vector κ_r and matrix R_r represent respectively the curvature and the rotation matrix at the last completed iteration. Matrix G is defined as follows:

$$G = \frac{4}{4 + g \cdot g}\left(I + \frac{1}{2} g\times\right)$$

and thus depends on the finite rotation from the reference frame at the last iteration to that at the running one. In the material frame, the elastic curvatures are:

$$\tilde{\kappa} = R^T G g' + R_r^T \kappa_r$$

and only the first addendum on the right-hand side depends on the unknown rotation parameters both in matrices R and G.

Equilibrium

The node equilibrium equations are summarised in the following equation:

$$\mathcal{A} D \Psi = \mathcal{F} \tag{11}$$

where $\mathcal{A}$ is the so called "arms" matrix. Matrix $\mathcal{D}$ is block diagonal and contains the constitutive matrices of the sections at the evaluation points in the global frame; vector Ψ represents the generalised deformations at the same points. Vector $\mathcal{F}$ represents the imposed loads. Let roman and arab footers denote entities related to the two evaluation points and the three nodes of a beam element respectively. The above mentioned matrices take the following form:

$$\mathcal{A} = \begin{bmatrix} -I & 0 & 0 & 0 \\ (p_I - x_1)\times & -I & 0 & 0 \\ I & 0 & -I & 0 \\ -(p_I - x_2)\times & I & (p_{II} - x_2)\times & -I \\ 0 & 0 & I & 0 \\ 0 & 0 & -(p_{II} - x_3)\times & I \end{bmatrix} \tag{12}$$

being p, with roman footers, the positions of the evaluation points and x, with arab footers, the positions of the beam reference points. Matrix $\mathcal{A}$, Equation (12),

directly descends from finite equilibrium, Equation (8), where the left hand matrix U has been evaluated at points p_I, p_{II}. The constitutive matrix is known in the material reference frame and thus must be transformed in the current frame of each section. This can be accomplished by means of a generalised rotation matrix $\mathcal{R}$:

$$\mathcal{D} = \mathcal{R}\tilde{\mathcal{D}}\mathcal{R}^T$$

Matrix $\mathcal{R}_{(12\times12)}$ is block diagonal and is made of a stack of rotation matrices:

$$\mathcal{R} = \text{diag}\left(\left[\begin{array}{cccc} R_I & R_I & R_{II} & R_{II} \end{array}\right]\right)$$

where matrices R_I, R_{II} are the rotation matrices at the evaluation points. The left multiplying $\mathcal{R}$ matrix accounts for the transformation of internal forces from the beam section to the global reference frame at evaluation points. The right multiplying $\mathcal{R}$ matrix accounts for the transformation of generalised deformations at the evaluation points from the global to the beam section reference frame. Matrix $\tilde{\mathcal{D}}$ is:

$$\tilde{\mathcal{D}} = \left[\begin{array}{cc} \tilde{D}_I & 0 \\ 0 & \tilde{D}_{II} \end{array}\right] \tag{13}$$

where $\tilde{D}_I$, $\tilde{D}_{II}$ are the constitutive matrices at evaluation points, in the material reference frame. Generalised curvatures are:

$$\Psi = \left\{\begin{array}{cccc} \varepsilon_I & \kappa_I & \varepsilon_{II} & \kappa_{II} \end{array}\right\}^T$$

Equation (13) gives the possibility to account for the axial variation of the beam properties in a discrete manner. The external loads vector takes the following form:

$$\mathcal{F} = \left\{\begin{array}{c} \int_{\xi_1}^{\xi_I}\left(I - U^T(\xi) + U^T(\xi_1)\right)\tau\, d\xi \\ \int_{\xi_I}^{\xi_{II}}\left(I - U^T(\xi) + U^T(\xi_2)\right)\tau\, d\xi \\ \int_{\xi_{II}}^{\xi_3}\left(I - U^T(\xi) + U^T(\xi_3)\right)\tau\, d\xi \end{array}\right\}$$

and may be briefly indicated as $\mathcal{F} = \left\{\begin{array}{cccccc} F_1 & C_1 & F_2 & C_2 & F_3 & C_3 \end{array}\right\}^T$.

Discretisation

The reference points of the beam and the geometric nodes are linked by means of an offset f. Then the i-th reference point position is $p_i = x_i + R_i\overline{f}_i$, where x_i is the position of the i-th node, R_i is its rotation matrix and $\overline{f}_i$ is the offset in the

node reference frame. The position of an arbitrary point of the reference line may be interpolated from nodes positions by means of parabolic shape functions $N(\xi)$:

$$p\left(\xi\right) = N_i(\xi)\left(x_i + R_i\overline{f}_i\right) \tag{14}$$

where footer i refers to the i-th node and summation over repeated indexes is assumed. The same shape functions may be used to discretise rotation parameters g too:

$$g\left(\xi\right) = N_i(\xi)\, g_i$$

Arbitrary point deformations then are:

$$\varepsilon\left(\xi\right) = N_i'(\xi)\left(x_i + R_i\overline{f}_i\right) - R\left(\xi\right)\overline{p'} \qquad \kappa\left(\xi\right) = G\left(\xi\right) N_i'(\xi)\, g_i + R_\Delta\left(\xi\right)\kappa_r$$

There's no need to exploit the dependence of rotation matrices on parameters $g\left(\xi\right)$ since the finite volumes formulation requires only punctual evaluation of strains.

Linearisation of the Equilibrium Equations

The solution of the system requires the local linearisation of the equations with respect to the considered unknown entities, i.e. the perturbations of nodal displacement and rotation unknowns, Δx_i and Δg_i. Analytical linearisation of the equilibrium equations may be easily obtained, since no numerical integration takes place in the formulation of the finite volumes beam. It is tedious, particularly due to the cumbersome expressions of the rotation matrices. The following relations hold:

$$\begin{aligned}
\Delta x_j &= N_{jk}\Delta x_k \\
\Delta g_j &= N_{jk}\Delta g_k \\
\Delta R_j &= \left(G_j N_{jk}\Delta g_k\right) \times \left(R_r\right)_j \\
\Delta p_j &= N_{jk}\left(\Delta x_k - \left(R_r\overline{f}\right)_k \times G_k\Delta g_k\right) \\
\Delta\tilde{\varepsilon}_j &= \left(R_r\right)_j^T p_j' \times G_j N_{jk}\Delta g_k + R_j^T N_{jk}'\left(\Delta x_k - \left(R_r\overline{f}\right)_k \times G_k\Delta g_k\right) \\
\Delta\tilde{\kappa} &= \left(R_r\right)_j^T\left(G_j g_j'\right) \times G_j N_{jk}\Delta g_k + R_j^T\left(H\left(g_j'\right) N_{jk}\Delta g_k + G_j N_{jk}'\Delta g_k\right)
\end{aligned}$$

where footer j denotes the j-th evaluation point, while footer k denotes the k-th node. Matrix H derives from the relation $\Delta\left(Gg'\right) = \Delta G g' + G\Delta g'$ and represents the differentiation of matrix G. Linearisation of Equation (11) leads to:

$$\Delta\mathcal{A}\ \tilde{\Theta} + \mathcal{A}\ \Delta\tilde{\Theta} + \mathcal{A}\ \tilde{\Theta} = 0$$

The differentiation of matrix $\mathcal{A}$ is straightforward and involves the distance of the evaluation points p_I, p_{II} from the reference nodes:

$$\Delta\mathcal{A}_{ij}\ \vartheta_j = \left\{ \begin{array}{c} 0 \\ -t_j \times (\Delta p_j - \Delta x_i) \end{array} \right\}$$

The differentiation of the internal forces gives:

$$\Delta\vartheta_j = -\left\{ \begin{array}{c} (t_r)_j \times \\ (m_r)_j \times \end{array} \right\} G_j \Delta g_j + \left[\begin{array}{cc} R_j & 0 \\ 0 & R_j \end{array} \right] \tilde{D}_j \left\{ \begin{array}{c} \Delta\tilde{\varepsilon}_j \\ \Delta\tilde{\kappa}_j \end{array} \right\}$$

where the differentiation of the deformations has been previously exploited. The developed elastic terms contribute to the previously outlined multi-body dynamic system, which already accounts for lumped inertial contribution. The consistent (i.e. distributed) inertia forces require a numerical integration. Their linearisation isn't reported in this paper since they have't been implemented yet. For sake of completeness, the external loads should be linearised too, since the couples depend on the position due to the multiplication of forces times matrix U. No linearisation is required if only concentrated loads at the nodes are considered.

An Important Simplification: the Linear Case

The linearisation of the sole strains results in the important case of the linear formulation of the finite volumes beam. The linear strains are:

$$\varepsilon = p' + p_0' \times \varphi, \qquad \kappa = \varphi' \tag{15}$$

where φ represents the linearised rotation. The finite equilibrium equation, Equation (11), then becomes:

$$\left[\begin{array}{cccc} -I & 0 & 0 & 0 \\ -(p_I - x_1)\times & -I & 0 & 0 \\ I & 0 & -I & 0 \\ (p_I - x_2)\times & I & -(p_{II} - x_2)\times & -I \\ 0 & 0 & I & 0 \\ 0 & 0 & (p_{II} - x_3)\times & I \end{array} \right] \mathcal{D} \left\{ \begin{array}{c} \varepsilon_I \\ \kappa_I \\ \varepsilon_{II} \\ \kappa_{II} \end{array} \right\} = \left\{ \begin{array}{c} F_1 \\ C_1 \\ F_2 \\ C_2 \\ F_3 \\ C_3 \end{array} \right\} \tag{16}$$

Discretisation of Equations (15) is straightforward and gives:

$$\varepsilon = N_i' x_i + p_0' \times N_i \varphi_i - N_i' f_i \times \varphi_i, \qquad \kappa = N_i' \varphi_i$$

Thus the linear finite equilibrium relation, Equation (16) may be witten in terms of the constant stiffness matrix as follows:

$$\mathcal{A}D \begin{bmatrix} N'_{Ii} & p'_{0I} \times N_{Ii} - N'_{Ii} f_i \times \\ 0 & N'_{Ii} \\ N'_{IIi} & p'_{0II} \times N_{IIi} - N'_{IIi} f_i \times \\ 0 & N'_{IIi} \end{bmatrix} \begin{Bmatrix} x_i \\ \varphi_i \end{Bmatrix} = \mathcal{F}$$

where the arms matrix $\mathcal{A}$ and the constitutive matrix $\mathcal{D}$ have been previously defined. Matrix $\mathcal{D}$ as well as offsets f_i and initial derivatives of position vector, p'_{0I} and p'_{0II} are evaluated at the reference configuration, which is assumed to remain unchanged.

Numerical Results

Static Load of a Cantilever Beam

The proposed beam element formulation is able to determine the exact solution in terms of nodal displacements and internal forces when loaded at its ends. Let's consider directly the most meaningful case, represented by a transverse load applied at one end, the other being clamped. The exact solution for a linear C^0 beam with constant properties is represented by a third degree polynomial for the transverse displacement and a second degree polynomial for the section rotation, here written for unit force:

$$\begin{aligned} v &= \frac{1}{2}\frac{l}{GA}(\xi + 1) + \frac{1}{48}\frac{l^3}{EJ}\left(5 + 9\xi + 3\xi^2 - \xi^3\right) \\ \varphi &= \frac{1}{8}\frac{l^2}{EJ}\left(3 + 2\xi - \xi^2\right) \end{aligned}$$

where l is the length of the beam, EJ and GA are the bending and shear stiffnesses and ξ is a nondimensional abscissa ranging from -1, the clamped end, to 1, the free one. The proposed formulation uses second degree shape functions for both the displacement and the rotation, so it seems not to be able to describe the exact solution. Since the transverse force is constant, the shear strain must be constant too. When the parabolic shape functions are employed to interpolate the nodal values of the exact solution, the following relation is determined for the shear deformation $\gamma = v' - \varphi$:

$$\gamma = \frac{1}{GA} + \frac{1}{24}\frac{l^2}{EJ}\left(3\xi^2 - 1\right) \tag{17}$$

The exact value for the shear strain is $\gamma = 1/GA$, which may be obtained from the interpolated one when the last addendum of Equation (17) vanishes. This happens for $\xi = \pm 1/\sqrt{3}$, to which the chosen positions for the evaluation points correspond [14]. That is, the internal forces at these points assume their exact value, thus explaining why the exact solution for the nodal displacements is obtained. The fact that the mentioned points also correspond to the Gauss quadrature points for second and third degree polynomials should suggest some interesting considerations on the effectiveness of a collocated method when compared to its equivalent, but numerically evaluated, "energetic" ones.

Euler Critical Load

Buckling critical load due to a conservative axial force that compresses a bar is a classical benchmark for non-linear/linearised beams formulations. From the linear elasticity theory the value of the critical load is known to be:

$$P = \frac{\pi^2}{4}\frac{EJ}{l^2}$$

for a clamped-free beam. This solution is physically meaningful since the applied load is conservative [19]. The finite volumes linearised pre-stress matrix comes from the linearisation of the arms matrix, Equation (12), referred to a previously calculated pre-stress condition. The above mentioned linearisation leads to the following relation:

$$\mathcal{F}_0 = \begin{bmatrix} 0 & 0 & 0 & 0 \\ -(p_I - x_1)\times & 0 & 0 & 0 \\ 0 & 0 & 0 & 0 \\ (p_I - x_2)\times & 0 & -(p_{II} - x_2)\times & 0 \\ 0 & 0 & 0 & 0 \\ 0 & 0 & (p_{II} - x_3)\times & 0 \end{bmatrix} \begin{Bmatrix} t_{I0} \\ m_{I0} \\ t_{II0} \\ m_{II0} \end{Bmatrix}$$

Displacements at nodes and at evaluation points may be easily discretised by means of Equation (14), thus giving the following expression for the pre-stress stiffness

matrix:

$$K_p = \begin{bmatrix} 0 & 0 \\ t_{I0} \times (N_{Ii} - \delta_{i1} I) & -t_{I0} \times N_{Ii} f_i \times \\ 0 & 0 \\ \begin{pmatrix} -t_{I0} \times (N_{Ii} - \delta_{i2} I) \\ +t_{II0} \times (N_{IIi} - \delta_{i2} I) \end{pmatrix} & \begin{pmatrix} t_{I0} \times N_{Ii} f_i \times \\ -t_{II0} \times N_{IIi} f_i \times \end{pmatrix} \\ 0 & 0 \\ t_{II0} \times (N_{IIi} - \delta_{i3} I) & -t_{II0} \times N_{IIi} f_i \times \end{bmatrix} \begin{Bmatrix} x_i \\ \varphi_i \end{Bmatrix}$$

Explicit solutions for the critical load and the deformation shape have been derived for a straight, constant properties beam modelled by means of a single element with equally spaced nodes and loaded by an end-applied axial compression force. The evaluation points have been placed in Gauss' integration points for third degree polinomials, in order to obtain the exact solution for a beam statically loaded at its ends [14]. Two buckling modes have been found, whose critical values are:

$$P_{fv} = \frac{24}{5 \pm \sqrt{21}} \frac{EJ}{l^2} \tag{18}$$

The lower value gives an error of about 1.48%.

Dynamic simulations of the buckling condition have been performed by means of the multi-body implementation of the formulation. A static analysis has been performed, involving a slowly growing axial compression load; a transversal disturbance load has been used to slightly perturb the straight solution. An abrupt increase in the lateral deviation takes place when the axial load approaches the critical value. Subsequently, in order to determine whether the limit value of the axial load has been reached or not, the transversal disturbance is removed. As a consequence the beam tends to return to the straight position. If the critical value has been overcome, the beam remains bended even when the transversal load vanishes. The numerical simulations determined a lower and an upper limit for the critical value, due to the fact that when the exact value is approached, the Jacobian matrix of the system in the undeformed configuration becomes singular and the system doesn't converge to a physically meaningful solution. The lower and upper bounds obtained by means of a single element model exacly bound the analytic value given by Equation (18). The ones obtained by means of a 4 elements model are close to the exact value within a $\pm 0.04\%$ error, thus standing for the effectiveness of a still relatively coarse model. The beam, indeed, can resist a load that is larger than the critical one when

the full non-linear behaviour is taken into account. Nevertheless a large curvature is required in order to counteract the load which, in the bended configuration, is not axial any more, as shown in Figure 2. In this figure a four element beam carries a load up to twice the buckling critical value. Figure 3 shows the internal forces due to the 2 P_{cr} load, calculated at the evaluation points of the four beams.

Dynamics of an Helicopter Rotor Blade

This example deals with the analysis of the dynamics of a rotor blade. The availability of analytical and experimental data on vibration analysis of a free rotor blade, courtesy of Agusta, suggested the use of such a trial case to test the reliability of the proposed formulation [12]. The system consists in a metallic rotor blade, made of aluminum alloy, that was mounted on Agusta A109 commercial helicopter and has been subsequently replaced by a composite one. The blade is made of a 'C' shaped aluminium main spar, closed at his back by a rear spar. The whole structure is covered by an aluminium sheet and represents about one third of the chord. The back of the airfoil is honeycombed and is covered by a skin made of a thin aluminium sheet. The trailing edge is made of a 'V' shaped aluminium rib. A steel antiabrasive strip is put on the leading edge. Non-structural masses have been also taken into account, as well as glue and paint weight. Fourteen sections of the blade have been analysed. Every section has been characterised elastically and inertially by means of a dedicated finite elements code developed at this Department [1], [4]. The spars and the honeycomb have been modelled by means of brick elements, while two dimensional *laminæ* have been used for the skin and the antiabrasive strip. A three dimensional model was then generated, made of fifteen three-node beam elements. It is shown in Figure 4. A modal analysis of the model has been performed first by means of a linear finite volumes beam model. Both concentrated and consistent inertia forces have been used, in order to determine the influence of a less refined model on the results of the analysis. Subsequently the frequency response to a random load at one end of the blade in terms of internal forces has been determined by means of the Multi-Body code. The results of the spectral analyses are reported in Table 1. The proposed method seems to agree better with the experiment than the cited reference, but this comparison is not so significant. Only the very small difference between the calculated frequencies should be appreciated, due to the potential

differences between numerical models and experiment.

Ground Resonance of an Elastic Wind Mill

An elastic tower 7.5 m high carries a gear fairing 1 m long, on which a three blade articulated rotor is mounted. The inertial and stiffness properties of the system are described in Table 2. The tower carries a 50 kg concentrated mass. The rotor hub is represented by a 20 kg mass and rotates round a horizontal revolution hinge put at the free end of the fairing. Three blades are mounted on the hub with a 0.25 m offset. They can freely to rotate round the flap and lead-lag hinges, that are coincident, while the pitch is imposed. The blades span 5 m; both rigid and deformable blades have been considered. The tower is modelled by means of two three-node beam elements. The fairing uses one element only. Both the tower and the fairing share the same elastic and inertial properties. Output of internal forces is considered at the first evaluation point of the first beam element, that is at 0.792 m from the basement of the tower. Each deformable blade is modelled by means of two beam elements. The blade elastic and inertial properties are constant spanwise. Aerodynamic loads on the blades are taken into account. The blades have a constant spanwise chord of 0.25 m. A simple NACA 0012 airfoil with experimentally determined aerodynamic coefficients spanning 360 degrees of angle of attack is considered. Standard air density at zero altitude is considered, that is $\rho = 1.225\ kg/m^3$. Aerodynamic loads are modelled by means of the strip theory, with a correction for uniform rotor induced speed. Hyperbolic twisting is imposed, in order to obtain a constant angle of attack under the assumption of uniformly distributed induced speed. Two half span aerodynamic elements per blade are considered. The same aerodynamic discretisation has been used for both the rigid and the deformable blades. The twist is modelled by means of a parabolic interpolation along each aerodynamic element. The first two simulations are made in vacuum; the rigid blade rotor has an initial speed of 20 and 30 rad/s respectively, to which stable and ground resonance conditions correspond. To chech for the stability of the system, the rotating speed of blade # 1 is slightly perturbed ($\Delta\Omega = -0.01\ rad/s$). This causes th gravity center of the rotor to move from the rotor axis. In the first case the system responds with almost undamped but stable in-plane oscillations, as may be seen in Figure 5, where the internal moments in the tower are described. In

the second case the system is unstable and breaks down in a quickly diverging motion. The diverging unstable motion appears clearly from the internal oments in the tower shown in Figure 6. The integration never fails even if non-physical results are obtained: at least one of the blades rotates more than 180 degrees round the lead-lag hinge. The behaviour of the beams in case of instability is not significant since no damage evaluation is made and a purely linear steady constitutive law is considered. Anyway both the beam element and the integrator are robust enough to integrate the unstable system most of the times without failing. All the simulations are performed with a time step of 0.005 s. Slight numerical damping is added by means of a linearly A-stable implicit time step integrator that allows the imposition of the desired asymptotic value for the spectral radius. A value of 0.6 is used unless otherwise stated. Some trials with different time step and numerical damping have been made in order to estimate the accuracy of the results. Time steps up to 0.015 s have been tested, which resulted in little loss in accuracy in the unstable case when low numerical damping was used, i.e. $\rho_\infty = 0.6$. In the case of high numerical damping, instead, while at 0.002 s the loss was negligible, at 0.02 s it was quite high. It may be appreciated that for time steps of 0.002 s, 0.005 s and 0.01 s, the differences in the overall motion are quite slight, the more appreciable errors being in the high frequency motions that are negligible in the ground resonance. Only for 0.015 s time step the overall motion is considerably distorted. The internal forces in Figure 5 strongly depend on the time step for the high frequency motion, the more evident errors being due to the period distortion operated by the numerical integration. Again, only for 0.015 s time step the high frequency internal forces are appreciably cancelled in amplitude. The unstable motion depicted in Figure 6 is clearly dominated by the retreating lag frequency motion and it is correctly modelled by time steps up to 0.01 s when low numerical damping is considered (asymptotic value of the spectral radius 0.6). When a 0.015 s time step is considered, or when the spectral radius is 0.3 with a time step of 0.01 s or larger, the response is appreciably different from the reference one. Based on these considerations, it can be stated that the selected time step is adequate for the spectrum of the system under analysis. Subsequent simulations involve the presence of the airstream. In the third case, the simulation starts with the rotor at a stable speed of 20 rad/s, and an axial airstream speed of 20 m/s is applied. The pitch of the blades is set at 2 degrees,

to which a couple of about 1600 Nm corresponds when account is made of uniform induced speed. Then a couple proportional to the rotating speed is applied at the rotor hinge, to counteract the aerodynamic one. Initial oscillations caused by the untrimmed initial conditions may be appreciated in the very left side of Figure 7. They are quickly damped by the aerodynamic forces. During this transient phase the rotor blades assume the correct precone and lead-lag angles and the tower and the fairing bend and twist under the net traction and the aerodynamic couple of the rotor. Then, in a two seconds time, the airstream is raised up to 25 m/s, to which an unstable rotation speed of about 25 rad/s corresponds. The internal moments in this case can be found in Figure 8, while the divering motion can be appreciated from Figure 9, which shows the path of the hub in the plane of the rotor. If the air stream speed is put back at 20 m/s (4^{th} case) the system returns to a safe condition before the unstable motion reaches an appreciable amplitude; Figure 10 shows the internal moments in the above mentioned case. Figure 11 shows the flapping and the lead-lag angles, from which the history of the rotor can be clarly appreciated when the stable condition is recovered. Figure 7 show the hub rotation velocity versus time related to the two perturbed simulations for both the rigid and the deformable blade rotor. Since the rigid and the deformable blades share the same aerodynamic discretisation, the slight differences in their response are due to the aeroelastic effects that occur in the flexible model. All the simulations start abruptly at the nominal rotation speed, with both aerodynamic and inertial loads applied. Even if the initial configuration satisfies the constraint conditions, high frequency axial oscillations arise in the flexible blades, due to the centrifugal loads. Then physical damping in the axial direction only has been added to the blades by means of an adequate quasi-steady approximation of a viscoelastic constitutive law, namely $\vartheta = D\psi + E\dot{\psi}$ where $\dot{\psi}$ are the time derivatives of the true generalised strains. This efficiently damps away the oscillations in less than 0.2 s thus allowing a time saving abrupt start, with little loss in accuracy only in the very first part of the simulation.

Concluding Remarks

A new, easy to implement, efficient and computationally cheap beam formulation has been proposed, based on the Finite Volumes concept. The formulation has a strong physical sound since it can be cast to the direct writing of the equilibrium equations of a finite piece of beam. The formulation has been directly applied to arbitrarily curved and twisted beams subject to finite displacements and rotations. Finite volumes are considered in order to write the equilibrium equations of the finite beam. Then the dependance of the internal forces on the configuration is exploited. The forces must be evaluated only at the boundaries of the volumes, thus simplifying the generation of their contribution to the equilibrium equations. It has been proved that the equilibrium equations do not depend on the reference frame that is used to evaluate the internal forces and the strains. Consistent inertia forces have been considered as well as pre-stress conditions both in the linear (linearised) and non-linear case. A multi-body implementation has been described in detail, but without any loss in generality the finite volumes can be adapted to a wide variety of kinematic formulations. The proposed implementation gives a considerable freedom in the analysis by defining offsets from the reference points of the beam to the physical degrees of freedom, and independent reference frames for the beam sections in which the forces are calculated. The major drawback may be found in the intrinsic loss of symmetry in the stiffness matrix. Usually symmetry of the matrices is considered useful in traditional linear elastic analysis, but in more sophisticated problems such as non-linear and intrinsically non-symmetric analyses and specifically aero-servoelastic ones this is not the matter. Consistent instead of lumped inertia should be used if a coarse model is to be considered. Some classical benchmarks along with more sophisticated problems, such as modal analysis and non-linear time step simulations of real models, have been presented in order to demonstrate the soundness of the formulation.

References

[1] Giavotto, V., Borri, M., Mantegazza, P., Ghiringhelli, G. L., Caramaschi, V., Maffioli, G. C., and Mussi, F., "Anisotropic Beam Theory and Applications", *Computer & Structures*, Vol. 16, No. 1–4, 1983

[2] Bauchau, O. A., "A Beam Theory for Anisotropic Material", *J. Appl. Mech.*, N. 52, 1985, pp. 416–422

[3] Hodges, D. H., Atilgan, A. R., Cesnik, C. E. S., and Fulton, M. V., "On a Simplified Strain Energy Function for Geometrically non Linear Behaviour of Anisotropic Beams", *Composites Engineering*, Vol. 2, Nos. 5–7, 1992

[4] Ghiringhelli, G. L. and Mantegazza, P., "Linear, Straight and Untwisted Anisotropic Beam Section Properties From Solid Finite Elements", *Composites Engineering* Vol. 4, N. 12, 1994

[5] Borri, M., Ghiringhelli, G. L., and Merlini, T., "Linear Analysis of Naturally Curved and Twisted Anisotropic Beams", *Composites Engineering* Vol. 2, No. 5–7, 1992

[6] Bathe, K. J. and Bolourchi, "Large Displacement Analysis of Three-Dimensional Beams Structures", *Int. Journal for Numerical Methods in Engineering*, 1979, Vol. 14

[7] Borri, M. and Merlini, T., "A Large Displacement Formulation For Anisotropic Beam Analysis", *Meccanica*, No. 21, 1986, pp 30–37

[8] Simo, J. C., "A Finite Strain Beam Formulation. The Three-Dimensional Dynamic Problem. Part I", *Computer Methods in Applied Mechanics and Engineering*, Vol. 49, North Holland, 1985

[9] Simo, J. C. and Vu-Quoc, L., "A Three-Dimensional Finite Strain Rod Model. Part II: Computational Aspects", *Computer Methods in Applied Mechanics and Engineering*, Vol. 58, North Holland, 1986

[10] Borri, M., and Bottasso, C., "An Intrinsic Beam Model Based on a Helicoidal Approximation-Part I: Formulation", *Int. J. for Num. Meth. in Engineering*, Vol. 37, 1994, 2267–2289

[11] Borri, M., and Bottasso, C., "An Intrinsic Beam Model Based on a Helicoidal Approximation-Part II: Linearization and Finite Element Implementation", *Int. J. for Num. Meth. in Engineering*, Vol. 37, 1994, 2291–2309

[12] Ghiringhelli, G. L., "On the Three Dimensional Behaviour of Composite Beams", *Composites Part B*, 28B, pp. 613–626, 1997

[13] Hughes, T. J. R., *"The Finite Element Method"*, Prentice Hall International Inc., 1987

[14] Masarati, P. and Mantegazza, P., "On the C^0 Discretisation of Beams by Finite Elements and Finite Volumes", *l'Aerotecnica Missili e Spazio*, Vol. 75, pp. 77–86, 1997

[15] Ghiringhelli, G. L., Mantegazza, P., and Masarati, P., "Numerical Modelling of Anisotropic Non Homogeneous Beams with Embedded Piezoelectric Sensors and Actuators", 7^{th} *International Conference on Adaptive Structures and Technologies*, Sept. 23–25, 1996, Rome, Italy

[16] Ghiringhelli, G. L., Masarati, P., and Mantegazza, P., "Multi-Body Aeroelastic Analysis of Smart Rotor Blades, Actuated by Means of Piezo-Electric Devices", *CEAS Int. Forum on Aeroelasticity and Structural Dynamics*, June 17–20, 1997, Rome, Italy

[17] Cardona, A., Geradin, M., Granville, D., RaeyMaekers, V., "Module d'Analyse de Mécanismes Flexibles MECANO", Ph.D. Thesis, Université de Liège, 1988

[18] Brenan, K. E., Campbell, S. L., and Petzold, L. R., "*Numerical Solution of Initial-Value Problems in Differential-Algebraic Equations*", North-Holland, New York, 1989

[19] Bolotin, V. V., "*Nonconservative Problems of the Theory of Elastic Stability*", Pergamon Press, Oxford, 1963

List of Symbols

$p : B \subseteq \Re \mapsto \Re^3$	reference line
$\xi \in B$	curvilinear abscissa on B
$\vartheta = \{t, m\}$	internal forces and moments 6×1
τ	distributed forces and couples 6×1
T	differential arm matrix 6×6
Π_s	strain power
R	orthonormal rotation matrix
$v \equiv \dot{p}$, $\omega \setminus \omega\times \equiv \dot{R}R^T$	velocity and angular velocity
$\psi = \{\varepsilon, \kappa\}$	deformations 6×1
D	beam section linear elastic constitutive matrix 6×6
$w(\xi)$	weight function, unit-valued inside $[a, b]$
$\delta(\xi)$	Dirac's impulse function
U	arm matrix, integral of matrix T
$\rho \setminus \rho\times = R'R^T$	geometric curvature
$\mathcal{M}$	beam section inertial matrix
φ	arbitrary rotation vector
g	modified Gibbs-Rodriguez rotation parameters
q	MBDyn nodal dofs. 9×1
x	position of a node
$e_i, i = 1, 3$	orthogonal unit vectors
$G \setminus (Gg')\times = R'R^T$	differential rotation matrix
$\mathcal{A}$	beam element arm matrix 18×12
$\mathcal{D}$	constitutive matrices at eval. points 12×12
Ψ	strains and curvatures at eval. points 12×1
$\mathcal{F}$	nodal forces and couples 18×1
$\mathcal{R}$	rotation matrices at eval. points 12×12
Θ	internal forces and moments at eval. points 12×12
f	offset from node to beam reference point
$N(\xi)$	shape functions

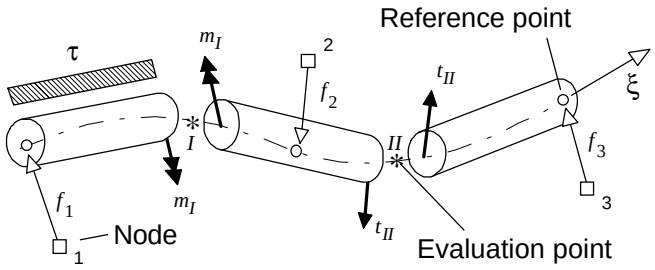

Figure 1: *Finite Volumes three-node beam*

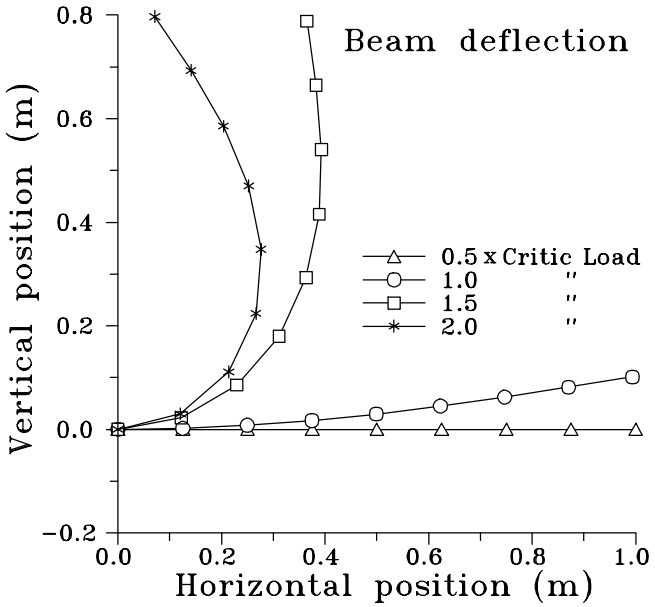

Figure 2: *Deformed shapes of a 4 three-node elements beam under 1, 3/2 and 2 times the critical buckling load*

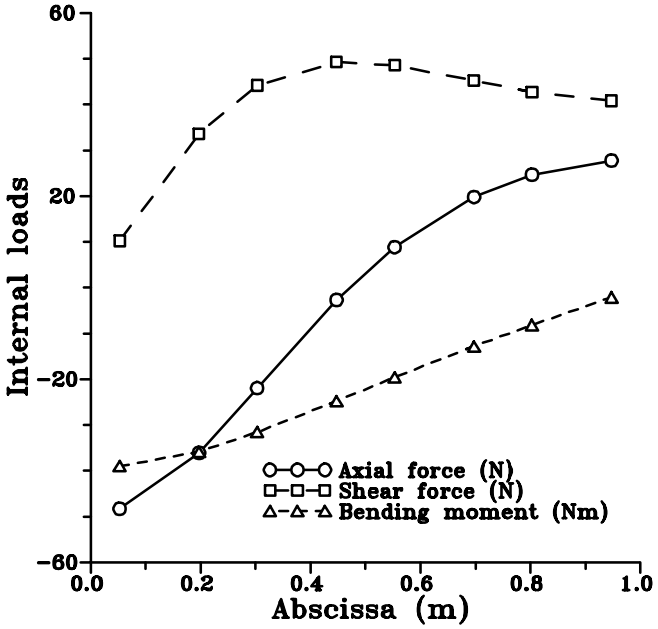

Figure 3: *Internal forces due to twice the critical buckling load, at the evaluation points of the four beam elements model*

Table 1: *Frequencies of a helicopter rotor blade*

Mode	Mode Type	Exper.	Ref. [12]	Lumped	Consist.
1	1 Beam	7.42	7.49	7.49	7.49
2	2 Beam	21.90	21.93	21.91	21.89
3	3 Beam	42.55	43.17	42.72	42.88
4	1 Chord	43.36	44.45	44.51	44.47
5	1 Torsional	65.70	66.35	68.32	66.22
6	4 Beam	70.81	73.34	72.64	72.62
7	5 Beam	105.78	110.20	107.51	107.85
8	2 Chord	121.97	125.34	125.69	125.57

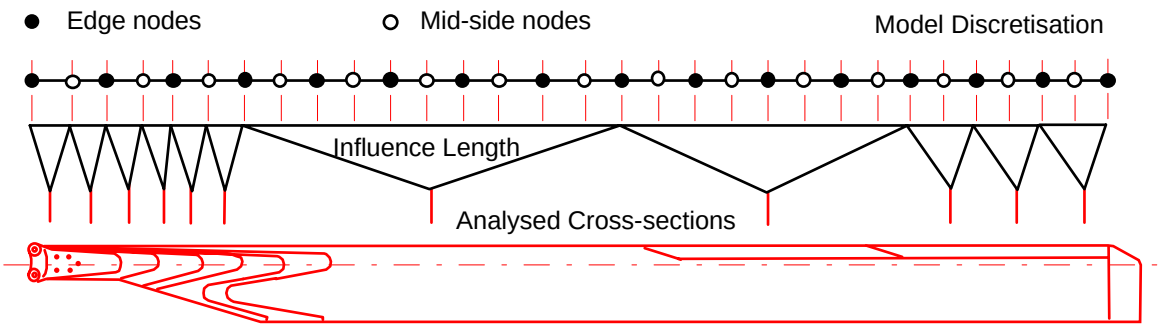

Figure 4: *Sketch of the dicretised helicopter blade*

Table 2: *Properties of the wind mill*

	Stiffness						Mass
	Axial	Shear, 2	Shear, 3	Torsional	Bending, 2	Bending , 3	
	N			$N \cdot m$			Kg/m
Tower	1.0×10^6	1.0×10^9	1.0×10^9	2.0×10^7	4.0×10^7	4.0×10^7	12.0
Fairing	1.0×10^6	1.0×10^9	1.0×10^9	2.0×10^7	4.0×10^7	4.0×10^7	12.0
Blades	1.0×10^6	1.0×10^7	1.0×10^6	1.0×10^6	1.0×10^5	1.0×10^4	3.0

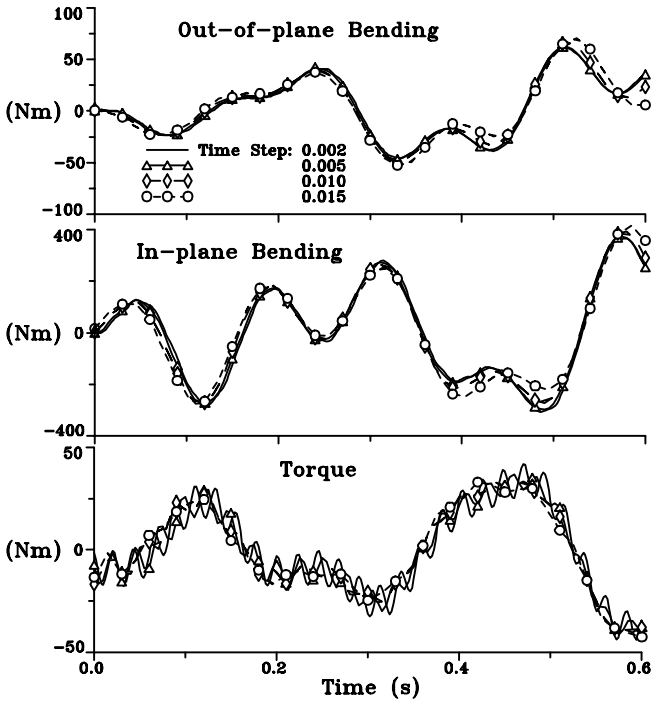

Figure 5: *Wind mill - internal forces in the tower, in-vacuum stable case* ($\Omega = 20\ rad/s$)

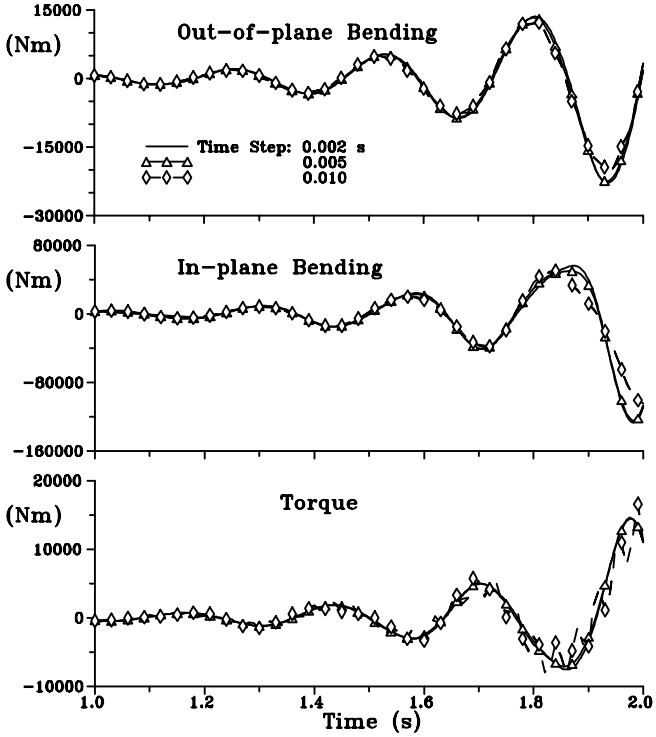

Figure 6: *Wind mill - internal forces in the tower, in-vacuum unstable case* ($\Omega = 30\ rad/s$)

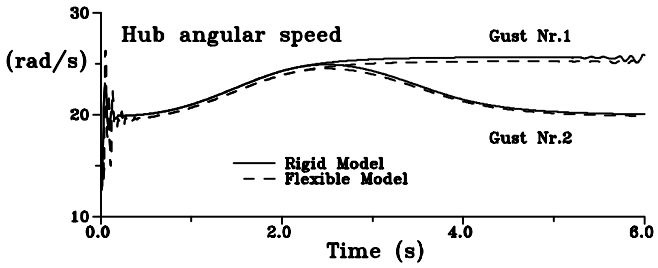

Figure 7: *Wind mill - velocity of the hub, in-air unstable and stable cases (gusts # 1 & # 2)*

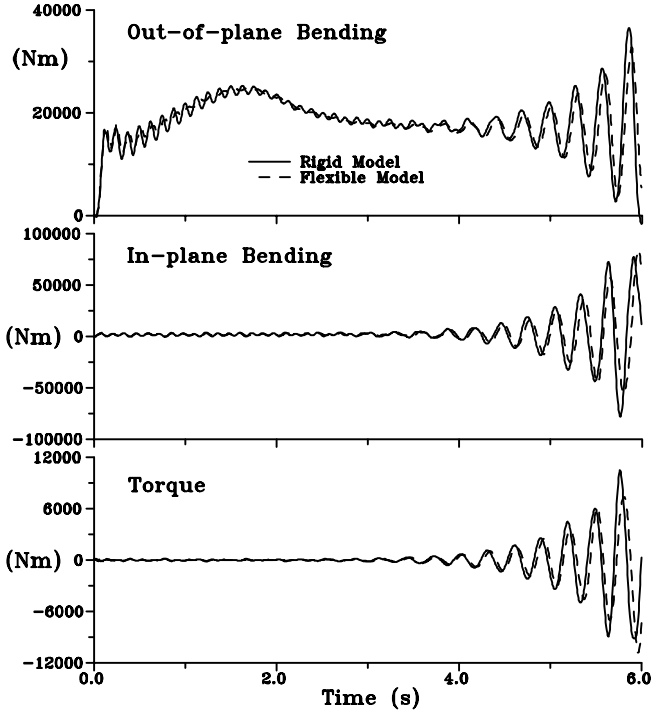

Figure 8: *Wind mill - internal forces in the tower, in-air unstable case (gust # 1)*

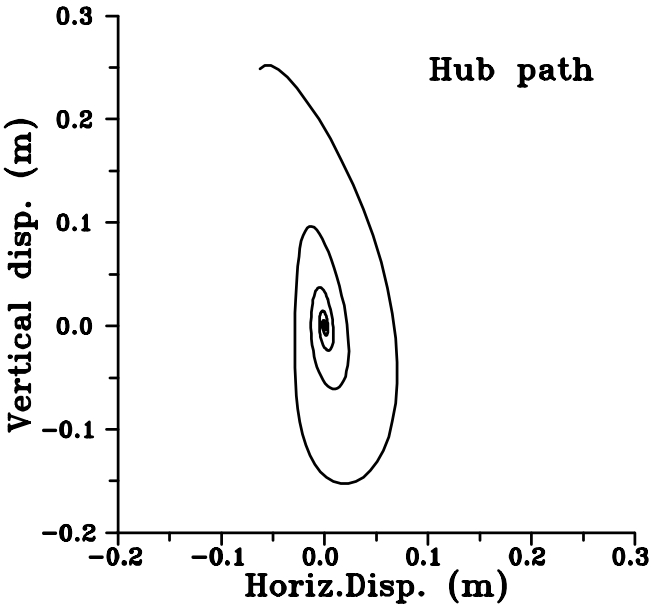

Figure 9: *Wind mill - path of the hub, in-air unstable case (gust # 1)*

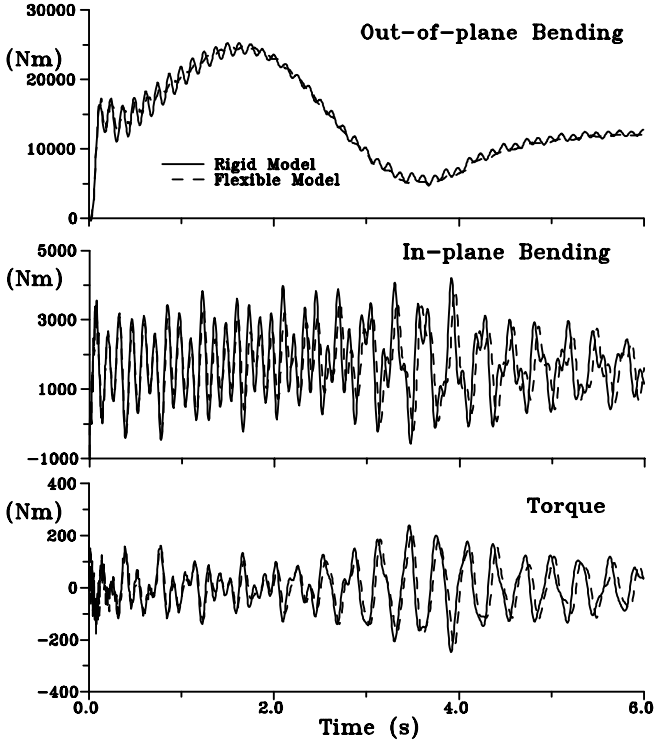

Figure 10: *Wind mill - internal forces in the tower, in-air stable case (gust # 2)*

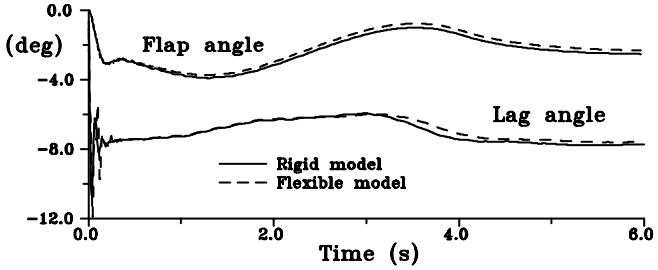

Figure 11: *Wind mill - flap and lead-lag angles, in-air stable case (gust # 2)*